NATIONAL BOARD FOR TECHNICAL EDUCATION
NIGERIAN JOURNAL FOR TECHNICAL EDUCATION
Volume 21 Nos. 1 2023
ISSN No. 2992 - 3522

Simultaneous Detection of Multiple Genuine and Counterfeited ₦500 and ₦1000 Banknotes in a Bunch **with Raman Spectroscopy: A Composite Raman Spectra Analysis of Substrate Longer Side**

Ahmed Murtala Kamba, Mutari Hajara Ali
BayeroUniversityKano, PhysicsDepartment(shugabamakamban1@gmail.com)
BayeroUniversityKano, PhysicsDepartment(mhali.phy@buk.edu.ng)

Abstract
Banknotes counterfeiting is a global problem that affects many currencies worldwide, including the Nigerian Naira note. However, the existing methods for counterfeit detectionusing Raman spectroscopy techniques are limited to single counterfeited noteidentification requiring multiple security features analysis. We proposed a novel approach requiring single security feature analysis to simultaneously detect multiple genuine and counterfeited Naira banknotes using Raman spectroscopytechnique and Multiview Nonnegative Matrix Factorization (MvNMF), increasing the detection efficiency from 1 to 36. By analyzing a sample bunch substrate on the longer side and using MvNMF to decompose the composite Raman spectra, the need for scanning various security features of each sample banknote can be eliminated, resulting in a significant increase in detection efficiency. This novel approach has the potential to be applied to other banknotes and security documents, such as passports, with distinct substrate spectral features, demonstrating the potential of Raman spectroscopy techniques in solving real-world problems related to document security.

Key words:- Naira banknote, Multiple counterfeits, Bunch, Raman spectroscopy, Multiview NMF, Longer side

1.0 INTRODUCTION

Despite the systematic printing measures by the engraving and printing agencies around the world to guarantee the security of genuine banknotes, counterfeiting is still a global problem that affect many countries' currencies including Nigeria Naira banknote. Usually, in counterfeiting production, criminals use similar specialized inks, papers and printers to produce fake copies of banknotes. A known scenario was Super-dollar and high-quality counterfeited currencies seized throughout the world. Their productions are usually in large quantity and within a shortest possible time and in most cases, they are hardly identified with ordinary eye. Duse to certain economic advantage and availability of material at the disposal of criminals, each country currency has its most counterfeited denomination. In Naira currency, ₦1000 and ₦500 banknotes denomination are the most counterfeited notes which account for 34.49% and 65.29% respectively. Most likely in Nigeria, criminals have three grades of fake notes which they produced. Generally, they paid more attention on quality of ink and prints of their fake notes as most important strategy. Their production has reached an extra ordinary level in quality and volume in some cases,which can be secretly deployed in to the economy by mixing them with genuine ones or directly deployed as a genuine mint

(fake mint). Recently, when new notes of ₦1000, N500, N200 and N100 was announce by the Nigerian government, huge amount of counterfeited note, especially N1000 and N500 were intercepted by the authorities. Authorities should therefore be on high alert for a possible deployment of large-scale counterfeited Naira notes when new notes were introduced and during political rallies for political ends.

Raman spectroscopy is a suitable photonic finger print method for analyzing molecules structure within material. Different molecules will have different Raman spectra. .Recently, Raman spectroscopy was applied in the literature for identification of forgeries in security documents , fiber orientation distribution analysis , molecular orientation analysis , molecular mapping , polarization anisotropy of a material and several other important information related to materials spectroscopy. In micro-Raman spectroscopy analysis, a Raman spectra finger prints of some selected security inks or Raman image of some selected security prints of fake notes were detected and distinguish with the Raman spectral information of genuine notes, leading to identification of differences in their chemical constituent or spectral images that establishedsingle counterfeited banknotes in each analysis .Micro-Raman spectroscopy was also successfully applied in establishing connection between different specimens of counterfeited banknotes, suspected to be printed with the same toner on the same printer . However in a related research but with different techniques other

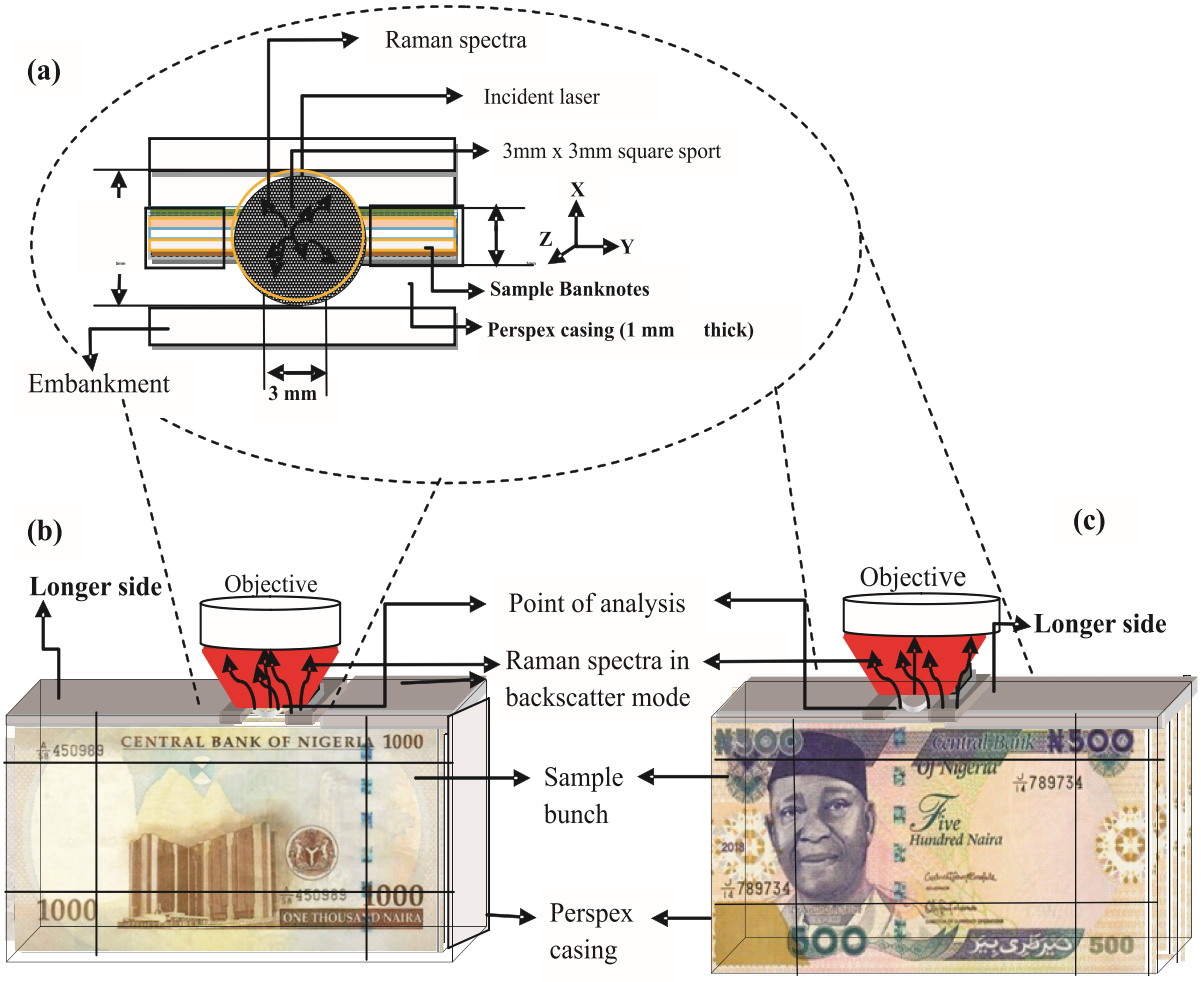

Figure 1. (a) Surface views of points of analysis under Raman probe b) ₦1000 sample bunch in Perspex casing and c) ₦500 sample bunch in Perspex casing under Raman probe

2.0 METHOD

It would be difficult for counterfeiters to produce fake banknotes with exact substrate security features of genuine banknote and no two different Paper will have exactly same Raman spectra . This research is based on simultaneous identification of overall Raman spectra finger prints of substrate spectra of each sample note within a bunch with both genuine and fake note (Fig. 1b & c) under same condition. Genuine and counterfeited ₦1000 and ₦500 note were collected, a homemade blank sample notes were also collected to form five sample bunches with different sample note arrangement (Table I). The composite Raman spectra result for each sample bunch was recorded in the rotational view between 0^0-180^0, for 45^0intervals to formed five corresponding matrices. Each matrix is of

Table I. Summary of sample bunch content and arrangements

Sample	Blank	Counterfeit	Genuine	Combination arrangement (Blank: 0, and Counterfeit: o, & Genuine: 1)
SAMPLE A PAPER-1	36	0	0	00000000000000000000000000000000000
SAMPLE B 1000-1	35	0	1	00000000000000000100000000000000000
SAMPLE C 500-1	34	0	2	00000000000000000110000000000000000
SAMPLE D 1000-2	29	3	4	0000000000001o11oo10000000000000000
SAMPLE E 500-2	32	2	2	00100000000000000o000010000000000o0

2.1 Sample preparation

A circulated Genuine sample of ₦1000 notes (151mm x 78 mm), ₦500 notes (151mm x 78 mm) and counterfeited representative samples were collected from bank teller, automatic teller machine (ATM) and Bureau de Change on loan or donation. Homemade unprinted copies (blank) each size 151mm x 78 mm were made with A4 commercial print paper (amazon brand) without any further preparation. The blank notes ware cut from A4 paper such that their longer and shorter sides were cut along the shorter and longer sides of the source A4 paper respectively. To evenly close-up gaps between each sample on the longer and shorter sides for sample analysis, we constructed a rectangular casing with transparent-Perspex material (1 mm thick) that suitably contain the sample bunch and provide it with equal and opposite pressure on both sides forming a rigid bunch (Fig. 1b & c). An opening (9mmx3mm) was allowed at the point of analysis on the longer side of the casing (Fig, 1b & c). At one of the shorter side an exit is allowed open, as a gate way for inserting and removing sample bunch in and out of the casing. Moreover, additional slab of Perspex was added on the four sides of the casing for additional reinforcement (embankment) from outside (Fig. 1a) which provide additional pressure from the two opposite sides of the sample bunch.

2.2 Sample bunch formation

The following sample bunches were form for the analysis without any further preparation

i. a bunch of 36 pieces of blank (P) sample notes with arrangement tag as; **SAMPLE A PAPER-1: 36P**

ii. a bunch of 36 pieces of sample notes with 1 Genuine ₦1000 note mixed with 35 blank (P) notes with arrangement tag as; **SAMPLE B 1000-1: 17P-1G-18P**

iii. a bunch of 36 pieces of sample notes

containing 2 genuine (G) ₦500 notes mixed with 34 blank (P) notes with arrangement tag as; **SAMPLE C 500-1: 17P-2G-17P**

iv. a bunch of 36 pieces of sample note containing 4 genuine (G) ₦1000 notes, 3 counterfeited (C) ₦1000 notes mixed with 29 blank (P) notes with arrangement tag as; **SAMPLE D 1000-2: 12P-1G-1C-2G-2C-1G-17P**

v. a bunch of 36 pieces of sample note with 2 genuine (G) ₦500 notes, 2 counterfeited (C) ₦500 notes mixed with 32 blank (P) notes with arrangement tag as; **SAMPLE E 500-2: 2P-1G-14P-1C-4P-1G-10P-1C-2P**

2.3 Experiment

2.3.1 Raman spectrometer settings

The experiment utilized a WITec Alpha 300R Raman spectroscopy machine equipped with WITec control 5 software that utilized confocal techniques to focus the excitation light (laser) with a Zeiss EC Epiplan Neofluar DIC 10X / 0.25 (10X magnification, 0.25 numerical aperture) microscope. The 532nm excitation source wavelength was provided by a 120mW power laser. The backscattered Raman spectra were detected with a multi-channel CCD detector that recorded a full Raman spectrum with 390 X 2600 pixels on the CCD in 20 accumulations over a period of 0.5 seconds. The built-in WITec algorithm, Shape 100, was used to remove cosmic rays, background spectrum, and smooth the spectrum in the average of 9 pixels.

2.3.2 Experimental procedure

The original plan was to position the samples as shown in Figures 1b and c on the motorize stage of WITec Alpha 300R Raman spectroscopy machine. However, we encountered a problem when we discovered that the samples could not fit onto the motorized stage and beneath the microscopic objective of WITec Alpha 300R due to an insufficient gap between the objective and the stage. To address this issue, we temporarily folded the excess height on the opposite side of the analysis point for each sample, secured with a rubber band across the shorter side, and placed them onto the motorized stage. The microscopic objective was then able to focus the excitation light (laser) directly onto the 3mm x 3mm surface as shown in Figures 1b and c and the surface view can be seen in Figure 1a. To prevent saturation from fluorescence and minimize damage to the sample, the excitation power was reduced to 20mW. Raman spectral data were recorded in the range of -105.494 to 3735.177 /cm at each rotational position (Fig. 2), ranging from 0-180 degrees in 45-degree intervals, using a CCD with 390 by 2600 pixels. Each analysis was conducted with a 20-second acquisition time and 10 accumulations. Both spectral graphs and text data were recorded. Subsequently, Raman spectral data range between 57.417 to 3735.177/cm were use during the data analysis process.

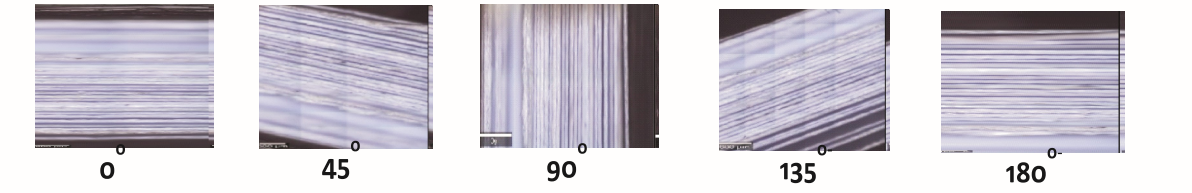

Figure 2. A 1700 μm captured surface view of the point of analysis in each rotational interval between 0-180 degrees.

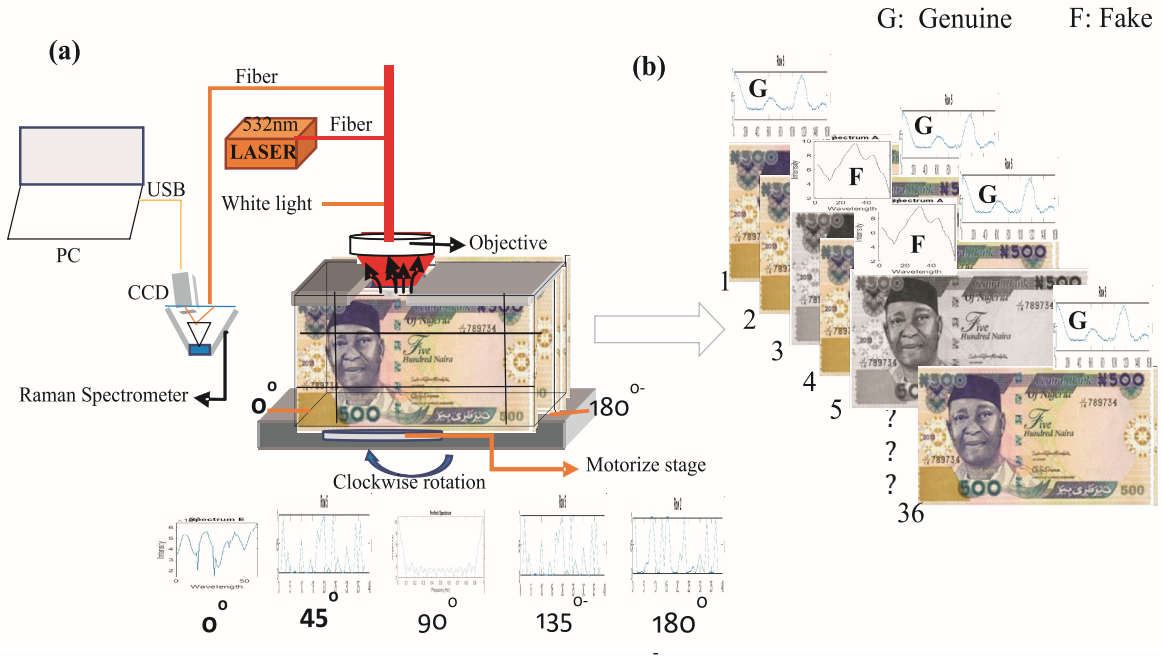

Figure 3. Experimental arrangement of the rotational acquisition scheme used in the detection of each bunch composite spectra

3.0 MODEL FORMULATION

According to spectra unmixing technique, the composite Raman spectra of the bunch detected by charge couple device is a linear combination of component spectra of individual sample note in the bunch. The sources of Raman intensities ii of these component spectra are thought to be from (Miron *et al.*, 2011) in each sample substrate. These sources are the molecules of micro fibrils of fibers (Svenningsson *et al.*, 2019; Workman, 2001; Zimmerley *et al.*, 2010) and the various components of the coating molecules (Bitla, 2002) that made up sample substrate. However, in this work the component spectra contribution of each sample notes in the composite spectrum of the bunch is a single overall spectrum of the sample which represent the combine spectrum of all the source molecules within the substrate of the sample note. This has eliminated the need for determining the number of sources in each sample which may likely be different for different sample note. In the rotational acquisition scheme, we use here, each composite spectrum of the *M* diverse angular rotation $\theta_1^{\cdots}\theta_M$, will have *K* wave numbers from single point. Depending on the Raman active molecules in the fiber and coatings of the substrate note relative to the linearly polarize laser plain of orientation, the depolarize composite-spectrum we detected will varies on each rotational orientation, though not much variation was observed since the detected spectra was a depolarize type.

Since each sample note in the bunch will contributes it overall sources spectra in the composite spectra of the bunch (Fig. 3), the composite data matrix of the bunch we acquire will be a weighted sum (superimposed spectra) (Zhang, Wang, Zhang & Li, ***2020)*** of the spectral data matrix of each sample banknote in the bunch. Each M^{th} recorded composite-Raman spectra of the bunch from the *M* diverse angular rotational points $\theta_1^{\cdots}\theta_M$ was concatenated to five rows of $v=5$ view with *MxK* dimensional data matrix ***DD*** In Machine learning, a renowned method of data decomposition known as Multiview Nonnegative Matrix Factorization (MvNMF) can be apply to decompose this composite data matrix into a product of two

lower dimensional matrices of their views as basis matrix $\boldsymbol{AA\ E\ R}^{MxN}$ which will contain the matrix result of Raman intensities as a function of rotational angle and the coefficient matrix $\boldsymbol{SS\ E\ R}^{KxN}$ (overall source matrix) as a function of wavenumber with a corresponding error estimate $\boldsymbol{EE\ R}^{MxN}$ given by (double alphabet indicate a bunch variable)

The two matrices factors are (Miron *et al.*, 2011):

$$\boldsymbol{AA} = \begin{pmatrix} ii_{1,}(\theta_1) \dots ii_{N,}(\theta_1) \\ \vdots \quad \dots \quad \vdots \\ ii_{1,}(\theta_M) \dots ii_{N,}(\theta_M) \end{pmatrix} \in \mathbb{R}^{M\times N}2$$

$$\boldsymbol{SS} = \begin{pmatrix} SS_{1,(\lambda_1)} \dots SS_{N,(\lambda_1)} \\ \vdots \quad \dots \quad \vdots \\ SS_{1,(\lambda_K)} \dots SS_{N,(\lambda_K)} \end{pmatrix} \in \mathbb{R}^{K\times N}3$$

The two equations (2 & 3) we obtained from Miron et al., (2011) work were modify to suit the depolarize data we detected in this work. Equation 2 & 3 were modified by removing the P subscripts (which indicated that data is a polarize spectra in X and Y) used in Miron et al., (2011) work.

Each column entries in the matrix (equation 2) represent the overal spetral intensity of each sample note in the various rotational angle. The row instensities entry represent the overal spectral intensity contribution of each sample note in the bunch in the specific rotational angle. The columns and rows of the coefficient matrix (equation 3) are the corresponding spectral coefficient of the columns and rows for the matrix of equation 2 respectively.

3.0.1. The Objective Function

Multiview objective function: To solve equation 1 using NMF minimization problem, we first obtain the objective function applying Frobenius norm which minimize the error

$$\underset{s.t\ \boldsymbol{DD,AA,SS} \geq 0}{minimize} \ \|\boldsymbol{DD} - (\boldsymbol{AA})(\boldsymbol{SS})^T\|_F^2 \quad 4$$

Where, $\boldsymbol{DD, AA, SS} \geq 0$ are nonnegative constrains to be satisfied for the minimiza of equation 1 and $\|.\|_F^2$ is a square Frobenius norm.

Equation 4 is standard objective function proposed by Daniel & Seung(1999) hat can structure the solution of matrix data as a whole entity, limiting it to single component (Wang et al., 2012) . This means that, the NMF minimization solution of this objective function will view the multi view Raman spectra collected as a homogeneous single view spectrum. However, the rotational (Multiview) scheme use in the data collection of this research must reflect the diverse views of the overall spectra of each banknote. In machine learning, diversity require that any two data vectors be orthogonal to each other. This is achieved when their product is roughly equal to zero. *To explore this diverse information across the components views in the basis matrix and the coefficient matrix of equation 2 & 3, we enforce a multi view diversity parameter on the coefficient matrix* $\sum_{w=1,w\neq v}^{V} tr\left((\boldsymbol{SS})^{(v)}(\boldsymbol{SS})^{(w)^T}\right)$ which is generally use in unsupervised machine learning to guarantee the diversity of any two pair of different spectral view (vview & wview) of the data vector be diverse to each other.

$$s.t\ \underset{DD^{(v)}, AA^{(v)}, AA^{(w)}, SS^{(v)}, \alpha, \beta \geq 0}{minimize} \sum_{v=1}^{V} \left\| (DD)^{(v)} - (AA)^{(v)} (SS)^{(v)^T} \right\|_F^2 + \alpha \left\| (SS)^{(v)} \right\|_F^2 + \beta \sum_{w=1, w \neq v}^{V} tr\left((SS)^{(v)} (SS)^{(w)^T} \right) 5$$

The first and second term are rank approximation term, are regularization parameter that ensure smooth balance between the parameter term and the errors as well (Cheng *et al* ., 2010; Tian & Zhang, 2022) The third term (SS(v)SS(w)T)is the diversity is the diversity regularization term for the diverse spectral view recorded in the angular diversity scheme.
this will ensure diversity between any two recorded vectors to be divers to each other is orthogonal to each other, hence enforcing component diversity.

$$s.t\ \underset{DD^{(v)}, AA^{(v)}, AA^{(w)}, SS^{(v)}, \alpha, \beta \geq 0}{minimize} \sum_{v=1}^{V} \left\| (DD)^{(v)} - (AA)^{(v)} (SS)^{(v)^T} \right\|_F^2 + \alpha \left\| (SS)^{(v)} \right\|_F^2 + \beta \sum_{w=1, w \neq v}^{V} tr\left((SS)^{(v)} (SS)^{(w)^T} \right) 6$$

$$= tr\Big((DD)^{(v)} (DD)^{(v)^T} - 2(DD)^{(v)} \left((SS)^{(v)} (AA)^{(v)^T} \right) + \left((AA)^{(v)} (SS)^{(v)^T} \right) \left((SS)^{(v)} (AA)^{(v)^T} \right) \Big) + \alpha\, tr\left((SS)^{(v)} (SS)^{(v)^T} \right) + \beta \sum_{w=1, w \neq v}^{V} tr\left((SS)^{(v)} (SS)^{(w)^T} \right) \quad 7$$

3.0.2 OPTIMIZATION PROBLEM

The objective function (equation 5) is not convex on both $(AA)^{(v)}$ and$(SS)^{(v)}$variables simultaneously. That is, it cannot converge to a local minimum so as to have global minimum. Therefore, we use algorithm to find the local minima that can iteratively update $(SS)^{(v)}$ with $(AA)^{(v)}$fix,followbyupdating $(AA)^{(v)}$keeping $(SS)^{(v)}$fix.

In order to constrain each $\left[ii_{N,}(\theta_M)\right]_{pq} \geq 0$ and $\left[ss_{N,(\lambda_K)}\right]_{pq} \geq 0$ variables in the nonnegative problem of equation 7, we let $\omega_{pq}^{(v)}$ *and* $\delta_{pq}^{(v)}$ to be their respective Lagrange multipliers that $\omega^{(v)} = [\omega_{pq}^{(v)}]$ and $\delta^{(v)} = [\delta_{pq}^{(v)}]$. We find the Lagrange function $\mathcal{L}\left((AA)^{(v)}, (SS)^{(v)}\right)$of equation 7 for the minimization procedure as

$$\mathcal{L}\left((AA)^{(v)}, (SS)^{(v)}\right) = tr\Big((DD)^{(v)} (DD)^{(v)^T} - 2(DD)^{(v)} \left((SS)^{(v)} (AA)^{(v)^T} \right) + \left((AA)^{(v)} (SS)^{(v)^T} \right) \left((SS)^{(v)} (AA)^{(v)^T} \right) \Big) + \alpha\, tr\left((SS)^{(v)} (SS)^{(v)^T} \right) + \beta \sum_{w=1, w \neq v}^{V} tr\left((SS)^{(v)} (SS)^{(w)^T} \right) + tr\left(\omega_{pq}^{(v)} (AA)^{(v)} \right) + tr\left(\delta_{pq}^{(v)} (SS)^{(v)} \right) \quad 8$$

At local minima, we set the derivative of $\mathcal{L}\left((\boldsymbol{AA})^{(v)}, (\boldsymbol{SS})^{(v)}\right)$ (equation 8) with respect to $(\boldsymbol{AA})^{(v)}$ and $(\boldsymbol{SS})^{(v)}$ to be 0 for each we've

$$\frac{\partial \mathcal{L}\left((\boldsymbol{AA})^{(v)}, (\boldsymbol{SS})^{(v)}\right)}{\partial (\boldsymbol{AA})^{(v)}}$$

$$= \frac{\partial tr(\boldsymbol{DD})^{(v)}(\boldsymbol{DD})^{(v)^T}}{\partial (\boldsymbol{AA})^{(v)}} - 2\frac{\partial tr(\boldsymbol{DD})^{(v)}\left((\boldsymbol{SS})^{(v)}(\boldsymbol{AA})^{(v)^T}\right)}{\partial (\boldsymbol{AA})^{(v)}}$$

$$+ \frac{\partial tr\left((\boldsymbol{AA})^{(v)}(\boldsymbol{SS})^{(v)^T}\right)\left((\boldsymbol{SS})^{(v)}(\boldsymbol{AA})^{(v)^T}\right)}{\partial (\boldsymbol{AA})^{(v)}} + \boldsymbol{\alpha}\frac{\partial\, tr\left((\boldsymbol{SS})^{(v)^T}(\boldsymbol{SS})^{(v)}\right)}{\partial (\boldsymbol{AA})^{(v)}}$$

$$+ \beta\frac{\partial \sum_{w=1,w\neq v}^{V} tr\left((\boldsymbol{SS})^{(v)^T}(\boldsymbol{SS})^{(w)}\right)}{\partial (\boldsymbol{AA})^{(v)}} + \frac{\partial\, tr\left(\omega_{pq}^{(v)}(AA)^{(v)}\right)}{\partial (\boldsymbol{AA})^{(v)}}$$

$$+ \frac{\partial tr\left(\delta_{pq}^{(v)}(\boldsymbol{SS})^{(v)}\right)}{\partial (\boldsymbol{AA})^{(v)}} \qquad 9$$

$$0 = -2\left((\boldsymbol{SS})^{(v)}\right)(\boldsymbol{DD})^{(v)} + 2\left((\boldsymbol{AA})^{(v)}(\boldsymbol{SS})^{(v)^T}\right)\left((\boldsymbol{SS})^{(v)}\right) + \omega_{pq}^{(v)} \qquad 10$$

$$\omega_{pq}^{(v)} = 2\left((\boldsymbol{SS})^{(v)}\right)(\boldsymbol{DD})^{(v)} - 2\left((\boldsymbol{AA})^{(v)}(\boldsymbol{SS})^{(v)^T}\right)\left((\boldsymbol{SS})^{(v)}\right) \qquad 11$$

Using Karush-Kuhn-Tucker (KKT) condition (Boyd & Vandenberghe, 2006) for the nonnegativity on $(\boldsymbol{AA})^{(v)}$we've

$$\omega_{pq}^{(v)}\left(\omega^{(v)}\right)_{pq} = 0 \qquad 12$$

Therefore, the update rule for equation 5 is

$$(\boldsymbol{AA})_{pq}^{(v)} = (\boldsymbol{AA})_{pq}^{(v)} \odot \frac{\left((\boldsymbol{DD})^{(v)}\left((\boldsymbol{SS})^{(v)}\right)\right)_{pq}}{\left(\left((\boldsymbol{AA})^{(v)}(\boldsymbol{SS})^{(v)^T}\right)\left((\boldsymbol{SS})^{(v)}\right)\right)_{pq}} \qquad 13$$

Where $\odot$ is element wise multiplication and $\div$ is element wise division

For the coefficient matrix of the views $(\boldsymbol{SS})^{(v)}$

$$\frac{\partial \mathcal{L}\left((\boldsymbol{AA})^{(v)},(\boldsymbol{SS})^{(v)}\right)}{\partial(\boldsymbol{SS})^{(v)}}$$

$$= \frac{\partial tr(\boldsymbol{DD})^{(v)}(\boldsymbol{DD})^{(v)^T}}{\partial(\boldsymbol{SS})^{(v)}} - 2\frac{\partial tr(\boldsymbol{DD})^{(v)}\left((\boldsymbol{SS})^{(v)}(\boldsymbol{AA})^{(v)^T}\right)}{\partial(\boldsymbol{SS})^{(v)}}$$

$$+ \frac{\partial tr\left((\boldsymbol{AA})^{(v)}(\boldsymbol{SS})^{(v)^T}\right)\left((\boldsymbol{SS})^{(v)}(\boldsymbol{AA})^{(v)^T}\right)}{\partial(\boldsymbol{SS})^{(v)}} + \boldsymbol{\alpha}\frac{\partial\, tr\left((\boldsymbol{SS})^{(v)^T}(\boldsymbol{SS})^{(v)}\right)}{\partial(\boldsymbol{SS})^{(v)}}$$

$$+ \beta\frac{\sum_{w=1,w\neq v}^{V} tr\left((\boldsymbol{SS})^{(v)^T}(\boldsymbol{SS})^{(w)}\right)}{\partial(\boldsymbol{SS})^{(v)}} + \frac{\partial tr\left(\omega_{pq}^{(v)}(\boldsymbol{AA})^{(v)}\right)}{\partial(\boldsymbol{SS})^{(v)}} + \frac{\partial tr\left(\delta_{pq}^{(v)}(\boldsymbol{SS})^{(v)}\right)}{\partial(\boldsymbol{SS})^{(v)}} \qquad 14$$

Similarly, we've the update rule for the coefficient matrix for the views $(\boldsymbol{SS})^{(v)}$

$$\left((\boldsymbol{SS})^{(v)}\right)_{pq} = \left((\boldsymbol{SS})^{(v)}\right)_{pq} \odot \frac{\left(2(\boldsymbol{DD})^{(v)^T}(\boldsymbol{AA})^{(v)}\right)_{pq}}{\left(2\left((\boldsymbol{SS})^{(v)}(\boldsymbol{AA})^{(v)^T}\right)(\boldsymbol{AA})^{(v)} + 2\,\boldsymbol{\alpha}(\boldsymbol{SS})^{(v)} + \beta\sum_{w=1,w\neq v}^{V}(\boldsymbol{SS})^{(w)}\right)_{pq}} \qquad 15$$

Table II. Join Multiview NMF algorism for the bunch composite spectral decomposition

ALGORITHM

1: INPUT; Data matrix DD = [D[1],.....D[5]]T,N, V, maximum number of iteration, $\boldsymbol{\alpha}$ and $\boldsymbol{\beta}$
2: Normalize DD
3: Initialize AA and SS randomly and then set as constant
4: For v = 1, 2.... V do
5: Iterate until convergence or maximum iteration
6: Update coefficient matrix SS using equation 15
7: Update basis matrix AA using equation 13
8: Normalize AA and SS to have unit L2-norm columns
9: OUTPUT: Estimate of AA, SS and the spectral matrices of each sample banknote in the bunc

3.1 2D CO-VARIENCES AND CORRELATION OF MULTIVIEW SPECTRAL MATRIX

A 2D covariances and correlation of Multiview spectral-matrix of reference paper $\boldsymbol{A_P}$ against each n Multiview spectra-matrices of note in the bunch $\boldsymbol{B}_{C_n}$ are calculated. The 2-D column co-variances $Cov_h(\boldsymbol{A}_P, \boldsymbol{B}_{C_n})$,row co-variances $Cov_v(\boldsymbol{A}_P, \boldsymbol{B}_{C_n})$, column correlation $\boldsymbol{r_v}$, androwcorrelations $\boldsymbol{r_v}$ of the $M \times N$ matrices are given by (Dikbaş, 2017).

$$Cov_h(\boldsymbol{A}_P, \boldsymbol{B}_{C_n}) = \frac{\sum_M \sum_N \left(\boldsymbol{A}_{P_{MN}} - \overline{\boldsymbol{A}_{P_M}}\right)\left(\boldsymbol{B}_{C_{n_{MN}}} - \overline{\boldsymbol{B}_{C_{n_M}}}\right)}{M \times N} 16$$

$$Cov_v(A_P, B_{C_n}) = \frac{\sum_M \sum_N (A_{P_{MN}} - \overline{A_{P_N}})\left(B_{C_{n_{MN}}} - \overline{B_{C_{n_N}}}\right)}{M \times N} \quad 17$$

$$r_h = \frac{\sum_M \sum_N (A_{P_{MN}} - \overline{A_{P_M}})\left(B_{C_{n_{MN}}} - \overline{B_{C_{n_M}}}\right)}{\sqrt{\left[\sum_M \sum_N (A_{P_{MN}} - \overline{A_{P_M}})^2\right]\left[\sum_M \sum_N \left(B_{C_{n_{MN}}} - \overline{B_{C_{n_M}}}\right)^2\right]}} \quad 18$$

$$r_v = \frac{\sum_M \sum_N (A_{P_{MN}} - \overline{A_{P_N}})\left(B_{C_{n_{MN}}} - \overline{B_{C_{n_N}}}\right)}{\sqrt{\left[\sum_M \sum_N (A_{P_{MN}} - \overline{A_{P_N}})^2\right]\left[\sum_M \sum_N \left(B_{C_{n_{MN}}} - \overline{B_{C_{n_N}}}\right)^2\right]}} \quad 19$$

where $\overline{A_{P_M}}$, $\overline{B_{C_{n_M}}}$ and $\overline{A_{P_N}}$, $\overline{B_{C_{n_N}}}$ are the averages of M^{th} row and N^{th} column of matrix A_P and B_{C_n} respectively.

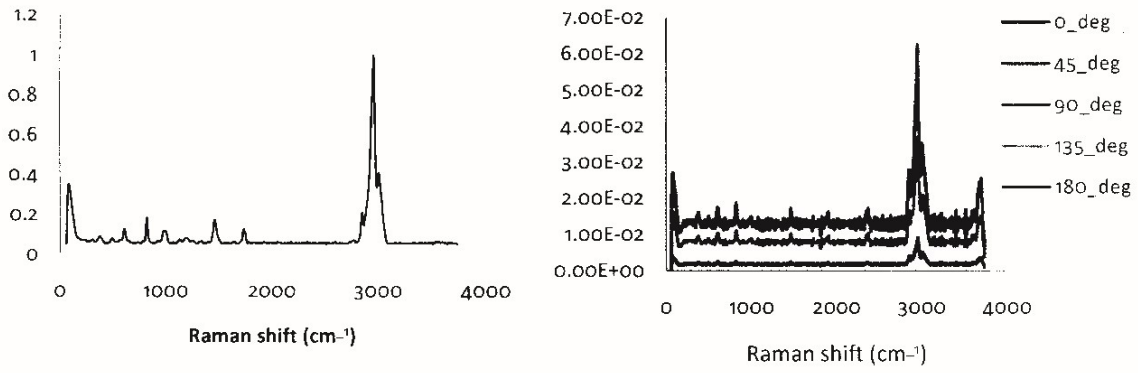

Figure 4. Experimental Perspex spectrum (single view) b) Decomposed Perspex spectrum (Multiview)

4.0 RESULTS

All the composite Raman spectra were detected and recorded for each of the five bunches. Sample A Paper-1: 36P was first decomposed and the overall Multiview Raman spectrum of the Perspex contribution (Fig. 4b) was extracted and subtracted from all composite Raman spectra matrices of the five bunches to obtain the pure Multiview data spectra. The pure data matrices were then decomposed, and the Multiview spectral-covariances and correlations between each sample note in the bunch and the Multiview spectra of the reference blank paper were calculated using equations 16, 17, 18, and 19, respectively, in the horizontal (rows) and vertical (columns) directions respectively.

4.0.1 Sample A PAPER-1: 36P

Table III presents the spectral results for vertical and horizontal covariance and correlations between the pure sample paper bunch and the reference blank paper spectra in SAMPLE A PAPER- 36P. Sample 4 exhibits the highest horizontal Multiview spectral-correlation of 0.95 to the reference blank spectra, while sample 22 has the lowest correlation of 0.03.

This table also highlights an interesting observation where all the samples are positively related in the horizontal direction (see Figure 5 also). This implies that the spectrum of each view in all samples in this bunch is positively similar to the reference blank paper spectra in the same view. Therefore, we can conclude that all samples in this bunch are blank paper as well. Additionally, Figure 5 demonstrates a scatter graph of the horizontal correlation, which displayed how the overall spectra view of each correlated set varies, indicating that even though the samples are from the same paper brand (Amazon) and are all blank, the spectra of some are more related to the reference spectra than others, both horizontally and vertically. This also indicates that same paper may have different spectrum in different rotational angle (view) under same analysis condition since paper is heterogenous complex material, although (Downes, 2019; Shin & Chung, 2013; Jones, Benson, & Roux, 2013) the difference may be small.

When we consider the overall intensities in different views, the samples in the blank bunch can covary and correlate positively or negatively. This is in contrast to the positive covariances and correlations (in the horizontal direction) observed in each view. The reason for this is that the variance of each view in the horizontal direction varies inversely due to difference in each view spectrum shape, resulting in negative covariances in the vertical direction for dissimilar spectrum and positive covariances for similar spectrum in different view. In simpler terms, the horizontal correlation measures the relationship between the overall spectral intensities of two sample spectra in each view. If the spectra are similar in each view, the result will be positive covariances and correlation, otherwise, it will be negative (except when the result is independent). While vertical correlation and covariance measure relationship between the overall spectral intensities of two sample spectra in different views. The vertical covariance and correlation results will be positive if the different view spectra are similar spectra are similar in each view. It is important to note that a zero covariance does not necessarily means that there is no relationship between the rows or columns of two spectral matrices sets, but could simply means that variability between the corresponding rows and columns is too low to detect a meaningful relationship

4.0.2 Sample B 1000-1: 17P-1G-18P

Table IV and Figure 6indicated that all samples in this bunch are positively correlated with the reference blank note except sample index 7 according to Multiview spectra localization.This sample is independently correlated (0 correlation) with the reference blank paper in the horizontal direction. This can also be verified in the bunch arrangement (TableI) as only one sample happens to be a counterfeit of ₦1000 Naira note in the bunch.

4.0.3 Sample C 500-1: 17P-2G-17P

Results of table V show two genuine ₦500 Naira note were independently correlated with the reference blank note, although they are not in both vertical covariance and correlation direction. The reason for that has already preceded in the previous section 4.0.1. The presence of two Genuine ₦500 note detected can be verify in the bunch analyzed (Table I). The scatter plot (Figure 7) of the horizontal correlation, have clearly indicated how all samples varies in the correlation.

4.0.4 Sample D 1000-2: 12P-1G-1C-2G-2C-1G-17P

In this sample results (Table VI), 3 samples

were independently correlated in the horizontal while 4 were negatively correlated to the reference MV spectra of the blank paper (see also Figure 8). The reason for this negative correlation and independent correlation in the horizontal could be attribute to presence sebum contamination on the surfaces of point of analysis in the genuine notes as some of the samples we collected were (section) already in circulation. Also, in this sample decomposition we observed increase in minimization error (Frobenious error: $\|\boldsymbol{DD} - (AA)(SS)^T\|_f^2$ to 3 digits. This however shows that four samples are the genuine ₦1000 notes (Table 1), while the 3 independently correlated sample are the counterfeits of ₦1000 note.

4.0.5 Sample E 500-2: 2P-1G-14P-1C-4P-1G-10P-1C-2P

This sample decomposition results in Table VII identify two samples as genuine ₦500 Naira note in the index of 4 and 7. These two detected samples number were exactly the same number of genuine ₦500 that were inserted in the actual sample bunch. These samples are the only sample identify to be independently correlated to the reference blank note (Table VII). This sample bunch contains two counterfeited ₦500 Naira note also, however the results indicated that they are positively correlated with the reference blank note also. This conclude that the substrate used in printing those fake note could be office paper with similar manufacturing chemical of the reference blank paper brand used (Amazon). One important conclusion that can also be derive from these results is that the same substrate is used in printing both genuine ₦500 and ₦1000 notes since both are independently corrected to the reference blank note.

Table III. Multiview spectral co-variation, correlation of each sample in the SAMPLE A PAPER-1: 36P bunch against the reference blank sample paper

A comparison between Blank Paper **Sample note**		cov_v	cov_h	r_v	r_h	**Sample Identity: Genuine note (1), Counterfeited note (o) and Blank note (0)**
Blank Paper	1	3.35E-05	2.64E-06	-0.44	0.07	o
	2	6.75E-05	4.73E-05	0.86	0.86	o
‘’	3	-2.11E-06	1.32E-05	-0.03	0.46	o
‘’	4	5.91E-05	3.50E-05	0.88	**0.95**	**o**
‘’	5	-3.50E-05	2.90E-06	-0.45	0.05	o
‘'	6	4.17E-05	2.33E-05	0.68	0.86	o
‘’	7	1.68E-05	2.36E-05	0.21	0.44	o
‘’	8	6.89E-05	4.88E-05	0.87	0.86	o
‘’	9	1.07E-05	2.08E-05	0.14	0.45	o
‘’	10	-1.45E-05	4.25E-06	-0.37	0.43	o
‘'	11	-3.98E-05	4.06E-06	-0.62	0.13	o
‘’	12	-1.82E-05	1.20E-05	-0.30	0.33	o
‘’	13	1.85E-06	8.32E-06	0.04	0.54	o
		-2.29E-	1.08E-	-		

‘’	14	05	05	0.35	0.27	0
‘’	15	1.69E-05	7.66E-06	0.62	0.81	0
‘’	16	-3.12E-05	3.58E-06	-0.42	0.10	0
‘’	17	-4.80E-06	1.32E-05	-0.08	0.45	0
‘’	18	-3.39E-05	1.83E-06	-0.43	0.04	0
‘’	19	-1.02E-05	1.28E-05	-0.17	0.40	0
‘’	20	-6.99E-06	9.16E-06	-0.13	0.46	0
‘’	21	-4.14E-05	2.80E-06	-0.67	0.11	0
‘’	22	-3.35E-05	1.30E-06	-0.42	0.03	0
‘’	23	1.84E-05	2.27E-05	0.26	0.55	0
‘’	24	-3.14E-05	6.19E-06	-0.48	0.19	0
‘’	25	1.77E-05	1.27E-05	0.31	0.67	0
‘’	26	-1.17E-06	1.60E-05	-0.02	0.49	0
‘’	27	-2.05E-05	1.11E-05	-0.29	0.25	0
‘’	28	5.01E-05	3.47E-05	0.73	0.85	0
‘’	29	-1.82E-8.12E-	7.48E-9.55E-	-	0.23	0

‘’	30	06	06	0.18	0.66	0
‘’	31	-3.70E-05	3.02E-06	-0.49	0.06	0
‘’	32	1.56E-05	2.30E-05	0.25	0.61	0
‘’	33	-2.48E-05	1.03E-05	-0.42	0.29	0
‘’	34	2.63E-05	1.53E-05	0.62	0.85	0
‘’	35	2.30E-05	2.42E-05	0.38	0.69	0
‘’	36	-1.32E-05	1.37E-05	-0.17	0.24	0

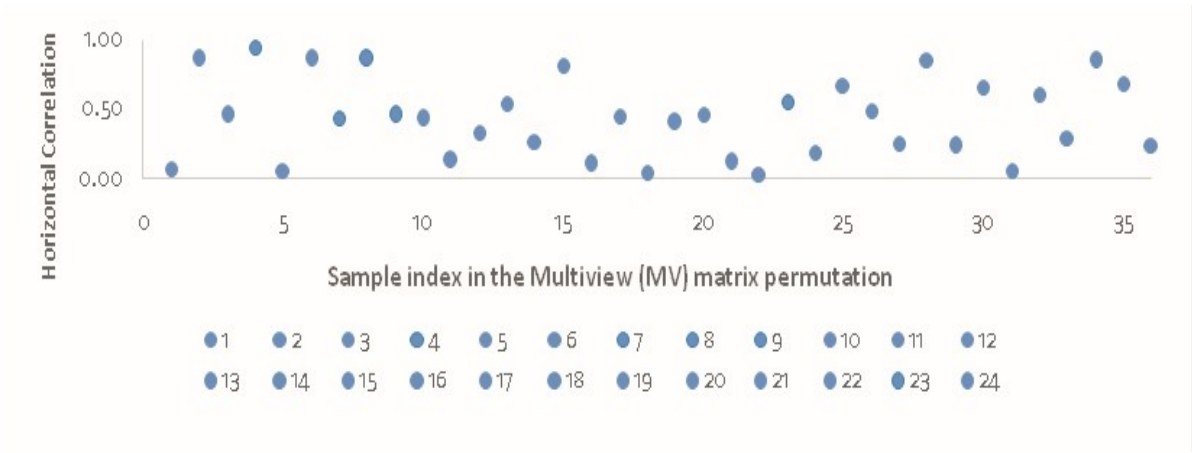

Figure 5. Scatter plot of sample A horizontal correlation (r_h)

Table IV. **SAMPLE B 1000-1: 17P-1C-18P bunch**: Multiview spectral co-variation, correlation and sample note location identification in the bunch

A comparison between Blank Paper **Sample note**		cov_v	cov_h	r_v	r_h	**Sample Identity: Genuine note (1), Counterfeited note (o) and Blank note (0)**
Blank Paper	1	8.96E-05	1.47E-05	0.97	0.80	0
‘’	2	-1.78E-05	1.85E-06	-0.18	0.06	0
‘’	3	2.21E-05	7.31E-06	0.33	0.47	0
‘’	4	-1.02E-05	4.20E-06	-0.12	0.17	0
‘’	5	-1.15E-05	3.26E-06	-0.12	0.09	0
‘'	6	1.80E-05	5.51E-06	0.24	0.41	0
‘’	7	-1.61E-05	8.78E-08	-0.16	**0.00**	**1**
‘’	8	-1.97E-05	7.93E-07	-0.20	0.02	0
‘’	9	-2.33E-06	7.10E-06	-0.03	0.25	0
‘’	10	2.08E-05	1.80E-06	0.42	0.42	0
‘'	11	2.40E-05	6.26E-06	0.32	0.42	0
‘’	12	2.11E-06	5.86E-06	0.03	0.28	0
‘’	13	1.99E-05	1.33E-06	0.42	0.33	0
‘’	14	-3.58E-06	5.15E-06	-0.04	0.23	0
‘’	15	-2.96E-06	1.55E-06	-0.73	0.15	0

‘’	15	-2.96E-05	1.55E-06	-0.73	0.15	0
‘’	16	9.11E-05	1.67E-05	0.96	0.81	0
‘’	17	-1.29E-06	3.81E-06	-0.02	0.27	0
‘’	18	9.25E-05	1.71E-05	0.96	0.81	0
‘’	19	-9.52E-06	3.39E-06	-0.14	0.21	0
‘’	20	-2.53E-06	3.24E-06	-0.05	0.33	0
‘’	21	2.58E-05	3.02E-06	0.45	0.46	0
‘’	22	9.45E-05	1.89E-05	0.96	0.81	0
‘’	23	-5.65E-06	5.92E-06	-0.07	0.25	0
‘’	24	3.98E-05	9.11E-06	0.48	0.54	0
‘’	25	3.51E-05	5.59E-06	0.50	0.52	0
‘’	26	-2.65E-05	2.66E-06	-0.40	0.13	0
‘’	27	-2.03E-05	2.41E-06	-0.24	0.08	0
‘’	28	-3.36E-05	9.83E-07	-0.45	0.05	0
‘’	29	8.51E-05	1.28E-05	0.96	0.78	0

‘’	30	-1.09E-05	2.75E-06	-0.19	0.26	0
‘’	31	1.58E-06	6.33E-06	0.02	0.22	0
‘’	32	-2.96E-05	1.85E-06	-0.40	0.08	0
‘’	33	-2.80E-05	8.59E-07	-0.33	0.03	0
‘’	34	-4.26E-05	7.07E-07	-0.88	0.05	0
‘’	35	-2.95E-05	1.77E-06	-0.44	0.11	0
‘’	36	-2.29E-05	1.09E-06	-0.25	0.03	0

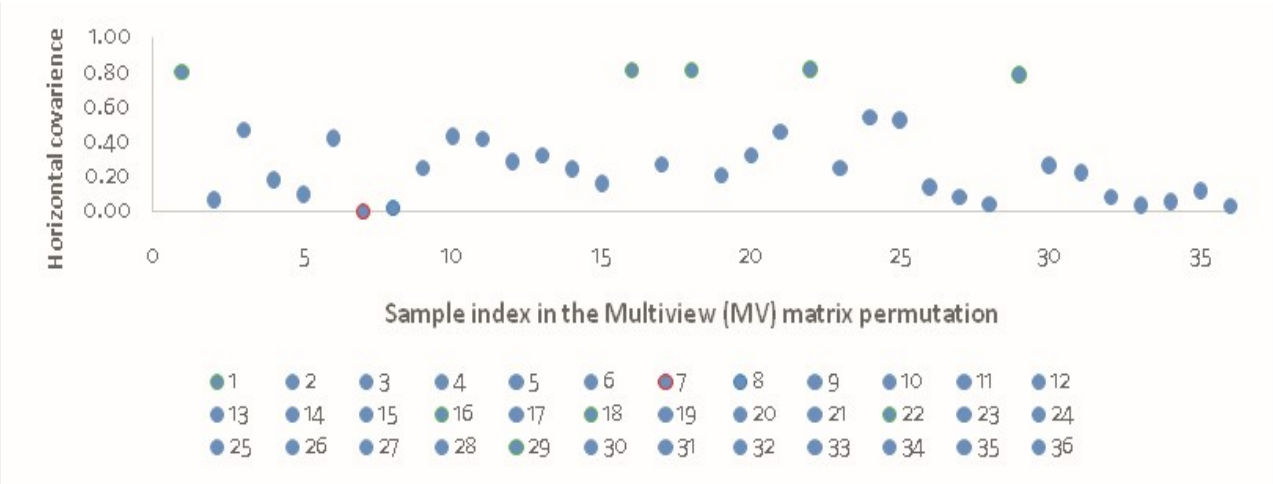

Figure 6. Scatter plot of sample B horizontal correlation (rh)

Table V. **SAMPLE C 500-1: 17P-2G-17P bunch**: Multiview spectral co-variation, correlation and sample note location (permutation) identification in the bunch

A comparison between Blank Paper **Sample note**		$\mathfrak{D}_{?}$	$\mathfrak{D}_{7}$	$?_{?}$	$?_{7}$	**Sample Identity: Genuine note (1), Counterfeited note (o) and Blank note (0)**
Blank Paper	1	7.70E-05	-2.63E-05	0.87	0.83	0
	2	-2.44E-05	4.66E-07	-0.38	0.04	0
''	3	1.22E-05	-3.57E-06	0.24	0.35	0
''	4	-1.11E-05	1.83E-07	-0.40	0.04	0
''	5	-1.89E-05	7.96E-07	-0.19	0.02	0
''	6	1.60E-05	-3.16E-06	0.43	0.37	0
''	7	-2.33E-05	1.72E-08	-0.24	0.00	1
''	8	-1.33E-05	1.46E-07	-0.13	0.00	1
''	9	-1.95E-05	3.78E-07	-0.21	0.03	0
''	10	3.83E-05	-1.32E-05	0.59	0.57	0
''	11	-1.77E-06	3.88E-06	-0.02	0.28	0
''	12	-2.30E-05	3.20E-06	-0.32	0.13	0
''	13	6.61E-05	-1.18E-05	0.92	0.77	0
''	14	-2.25E-05	2.82E-06	-0.27	0.09	0

‘’	15	1.52E-05	6.49E-06	0.37	0.46	0
‘’	16	5.55E-05	7.38E-06	0.71	0.58	0
‘’	17	-1.85E-05	2.93E-06	-0.25	0.16	0
‘’	18	7.45E-05	2.58E-05	0.85	0.80	0
‘’	19	-2.11E-05	1.42E-06	-0.34	0.16	0
‘’	20	2.21E-05	3.57E-06	0.84	0.53	0
‘’	21	2.93E-05	1.29E-05	0.38	0.49	0
‘’	22	8.19E-05	2.01E-05	0.89	0.79	0
‘’	23	-1.86E-05	3.64E-07	-0.20	0.02	0
‘’	24	-1.48E-05	6.44E-07	-0.15	0.01	0
‘’	25	3.15E-05	3.41E-06	0.52	0.35	0
‘’	26	-2.82E-05	8.78E-07	-0.47	0.09	0
‘’	27	-3.41E-05	5.54E-07	-0.43	0.04	0
‘’	28	-3.62E-05	6.79E-07	-0.51	0.03	0
‘’	29	4.61E-05	8.71E-06	0.66	0.54	0
‘’	30	2.10E-05	2.46E-06	0.79	0.49	0
‘’	31	-2.48E-05	1.27E-06	-0.31	0.09	0

‘’	32	-3.30E-05	6.46E-07	-0.47	0.05	0
‘’	33	-3.97E-05	3.74E-07	-0.56	0.03	0
‘’	34	-3.37E-05	9.06E-07	-0.85	0.11	0
‘’	35	-2.96E-05	1.14E-06	-0.38	0.04	0
‘'	36	-3.64E-05	2.63E-07	-0.47	0.02	0

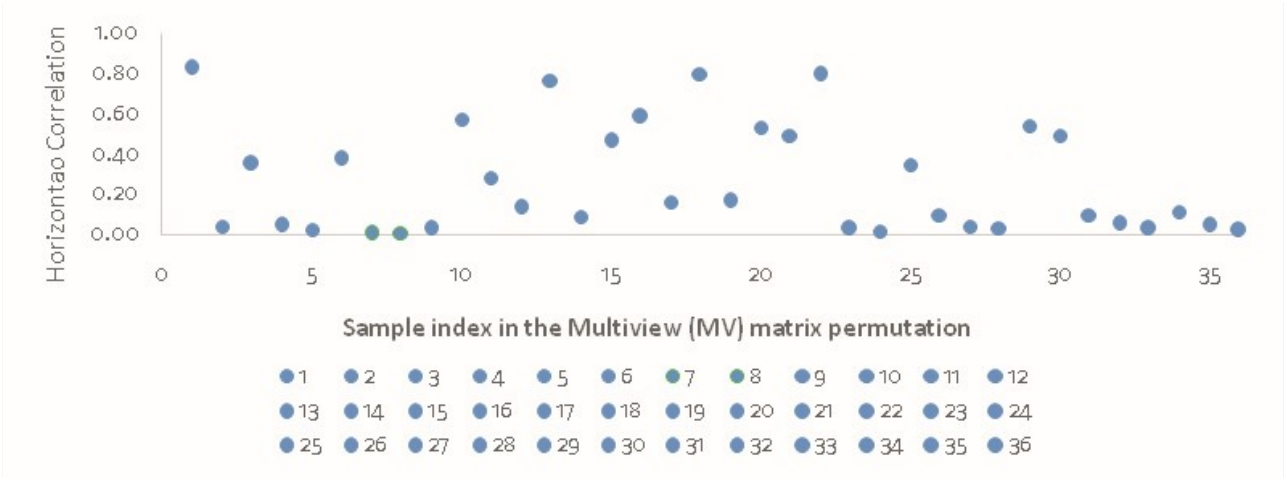

Figure 7 Scatter plot of sample C horizontal correlation (rh)

Table VI. **SAMPLE D 1000-2: 12P-1G-1C-2G-2C-1G-17P** Bunch: Multiview spectral co-variation, correlation and sample note location identification in the bunch

A comparison between Blank Paper **Sample note**		$\mathcal{D}_{?}$	$\mathcal{D}_{7}$	$?_{?}$	$?_{7}$	**Sample Identity: Genuine note (1), Counterfeited note (o) and Blank note (0)**
Blank Paper	1	6.13E-05	-4.07E-06	0.85	0.33	o
‘’	2	-2.31E-05	-2.08E-08	-0.25	**0.00**	**1**
‘’	3	-5.24E-06	3.62E-06	-0.08	0.29	o
‘’	4	-2.37E-05	5.53E-07	-0.35	0.09	o
‘’	5	-2.40E-05	1.41E-06	-0.28	0.06	o
‘'	6	-5.10E-06	-5.25E-07	-0.07	**-0.12**	**o**
‘’	7	-2.63E-05	1.34E-07	-0.27	0.01	1
‘’	8	-2.17E-05	-2.55E-08	-0.22	**0.00**	**1**
‘’	9	-2.05E-05	2.40E-06	-0.25	0.12	o
‘’	10	2.62E-05	1.43E-06	0.59	0.31	o
‘'	11	-1.03E-05	3.70E-06	-0.14	0.20	o
‘’	12	-	1.02E-	-	0.09	o

‘’	13	4.59E-05	1.17E-06	0.75	0.15	0
‘’	14	-2.38E-05	1.13E-06	-0.27	0.07	0
‘’	15	-6.41E-07	4.09E-07	-0.06	0.32	0
‘’	16	7.42E-05	1.28E-05	0.90	0.61	0
‘’	17	3.52E-06	2.80E-06	0.05	0.20	0
‘’	18	6.30E-05	7.67E-06	0.82	0.53	0
‘’	19	-1.92E-05	2.06E-06	-0.38	0.20	0
‘’	20	2.10E-05	4.94E-06	0.44	0.45	0
‘’	21	3.36E-05	7.14E-06	0.50	0.39	0
‘’	22	8.07E-05	1.10E-05	0.90	0.50	0
‘’	23	-2.73E-05	9.61E-07	-0.35	0.08	0
‘’	24	1.13E-06	3.13E-06	0.01	0.24	0
‘’	25	2.34E-05	-1.27E-07	0.31	-0.02	0
‘’	26	-3.18E-05	1.03E-06	-0.49	0.09	0
‘’	27	-3.85E-05	6.81E-07	-0.63	0.06	0
‘’	28	-	-4.41E-	-	0.01	0

29	1.98E-05	-5.71E-07	0.26	**0.10**	**0**
30	2.28E-05	3.42E-06	0.48	0.39	0
31	-2.64E-05	1.89E-06	-0.34	0.09	0
32	-3.41E-05	1.83E-07	-0.45	0.02	0
33	-4.07E-05	4.62E-07	-0.58	0.03	0
34	-3.57E-05	6.40E-07	-0.69	0.09	0
35	-3.09E-05	-2.69E-08	-0.42	**0.00**	**1**
36	-3.20E-05	2.50E-07	-0.37	0.02	0

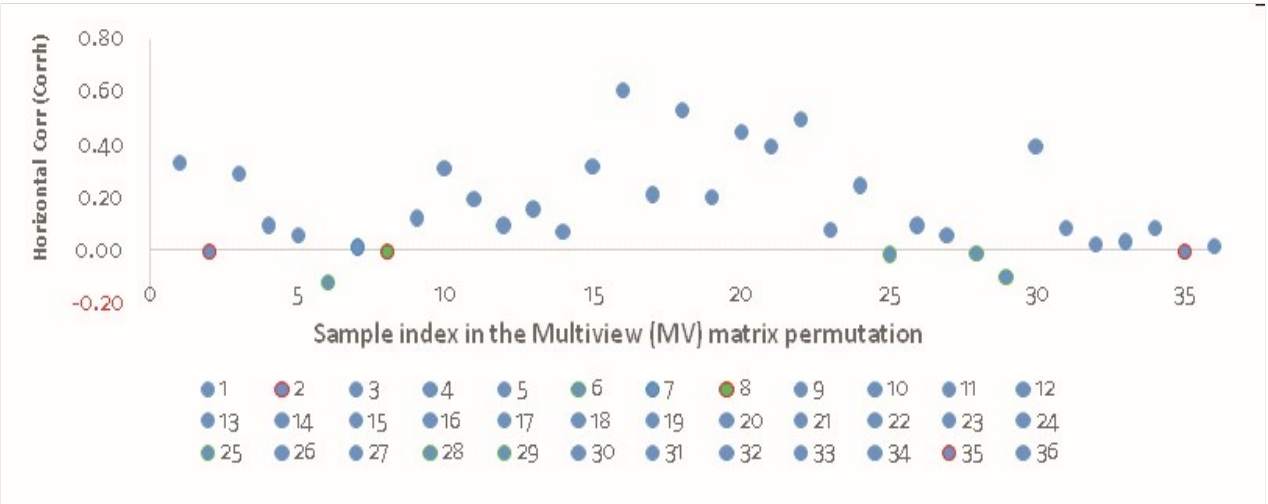

Figure 8. Scatter plot of sample D horizontal correlation (r_h)

Table VII. **SAMPLE E 500-2: 2P-1G-14P-1C-4P-1G-10P-1C-2P**Bunch: Multiview spectral co-variation, correlation and sample note location identification in the bunch

A comparison between Blank Paper **Sample note**		$\mathfrak{D}_{?}$	$\mathfrak{D}_{7}$	$?_{?}$	$?_{7}$	**Sample Identity: Genuine note (1), Counterfeited note (o) and Blank note (0)**
Blank Paper	1	8.26E-05	2.32E-05	0.92	0.84	0
''	2	-2.99E-05	5.55E-07	-0.39	0.03	0
''	3	1.28E-05	2.33E-06	0.22	0.31	0
''	4	-2.45E-05	3.96E-08	-0.37	0.00	1
''	5	-1.99E-05	1.14E-06	-0.20	0.03	0
''	6	7.81E-06	2.50E-06	0.16	0.26	0
''	7	-2.34E-05	8.84E-09	-0.24	0.00	1
''	8	-1.63E-05	2.18E-07	-0.16	0.01	0
''	9	-2.24E-05	1.11E-07	-0.23	0.01	0
''	10	4.78E-05	1.32E-05	0.68	0.62	0
''	11	3.17E-06	4.42E-06	0.04	0.31	0
''	12	-1.90E-05	3.46E-06	-0.26	0.15	0
''	13	7.38E-05	1.40E-05	0.95	0.81	0
''	14	-	2.77E-	-	0.11	0

‘’	15	1.21E-05	5.73E-06	0.28	0.44	0
‘’	16	5.39E-05	5.43E-06	0.68	0.53	0
‘’	17	-1.44E-05	3.32E-06	-0.18	0.17	0
‘’	18	7.93E-05	2.10E-05	0.91	0.80	0
‘’	19	-1.98E-05	1.76E-06	-0.28	0.17	0
‘’	20	3.03E-05	1.41E-06	0.74	0.44	0
‘’	21	3.90E-05	1.23E-05	0.50	0.56	0
‘’	22	8.41E-05	1.75E-05	0.92	0.80	0
‘’	23	-2.21E-05	1.06E-07	-0.23	0.01	0
‘’	24	-1.29E-05	2.83E-06	-0.13	0.07	0
‘’	25	9.94E-06	1.98E-06	0.15	0.17	0
‘’	26	-2.85E-05	5.18E-07	-0.40	0.06	0
‘’	27	-3.15E-05	6.51E-07	-0.38	0.04	0
‘’	28	-3.65E-05	6.35E-07	-0.50	0.03	0
‘’	29	5.03E-05	8.61E-06	0.72	0.59	0
‘’	30	1.50E-05	5.81E-07	0.39	0.15	0
‘’	31	-2.34E-05	1.35E-06	-0.28	0.10	0

‘'	31	-2.34E-05	1.35E-06	-0.28	0.10	0
‘’	32	-3.31E-05	6.00E-07	-0.43	0.04	0
‘’	33	-3.97E-05	3.30E-07	-0.57	0.03	0
‘’	34	-3.53E-05	1.82E-07	-0.87	0.04	0
‘’	35	-3.27E-05	1.17E-06	-0.45	0.05	0
‘'	36	-3.57E-05	2.42E-07	0.92	0.02	0

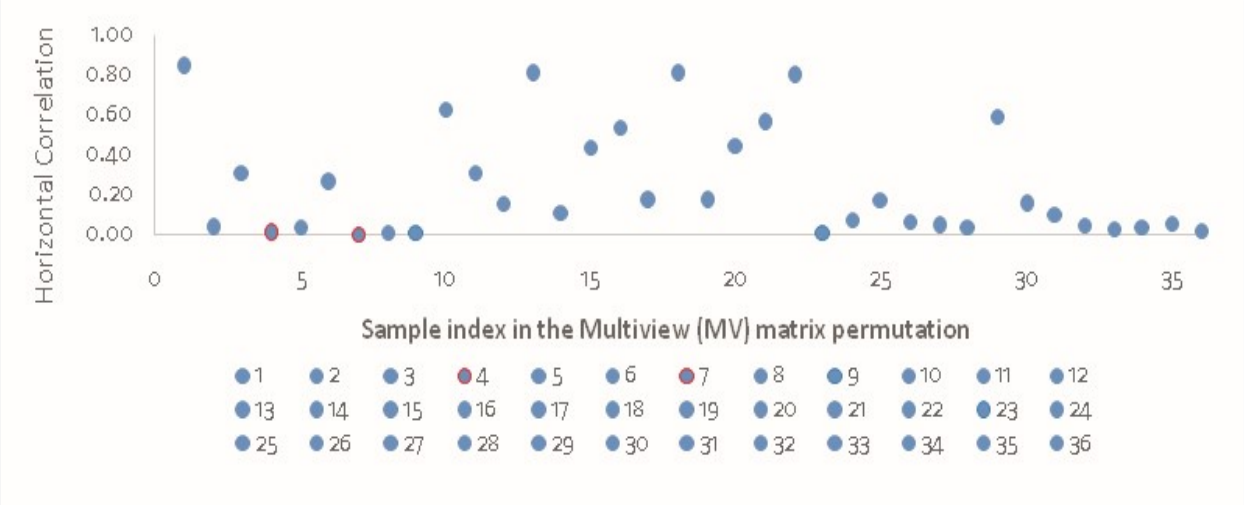

5.0 CONCLUSION

The research presents an efficient method for document security analysis, utilizing Raman spectroscopy to simultaneously detect multiple genuine and counterfeited ₦1000 and ₦500 Naira notes in a bunch. The approach eliminates the need for analyzing various security features to establish counterfeiting in Naira banknote which show the novelty of our proposed method. Our findings shows that samples of the same type have similar overall Raman spectra, whereas different samples exhibit distinct overall Raman spectra.Notably, presence of sebum contamination on the point of analysis could affect the overall Raman spectra results. This study does not address the localization of the decomposed samples within the bunch, this will be addressed in the feature research.

Overall, our research showcases the potential of Raman spectroscopy in combatting the presence of multiple counterfeit banknotes within a batch, offering significant benefits to government and financial institutions.

REFERENCES

Abu Doush, I., and AL-Btoush, S. (2017). Currency recognition using a smartphone: Comparison be tween color SIFT and gray scale SIFT algorithms. *Journal of King Sand University - Computer and Information Sciences* 29(4), 484 -492. https://doi.org/10.1016/jjksuci.2016.06.003

Bitla, S. (2002). Application of Raman Techniques for Paper Coatings Application of Raman Techniques.*Submitted in Partial Fulfillment of the Requirements for the Degree of Master of Science (In,* 1-69.)

Boyd, S., and Vandenberghe, L. (2006).

Convex Optimization %L'ikJ5&& (andN.

Anna, Nicholas & D. and Margriet (eds.); 2009th ed., Vo 1. 3, Issue 1). Cambridge University Press, https://web.stanford.edu/~boyd/cvxbook/bv_cvxbook.pdf

Bozicevic, M. S., Gajovic, A., and Zjakic, I. (2012). Identifying a common origin of toner printed counterfeit banknotes by micro -Raman spectroscopy. *Forensic Science International,* 225(1-3), 314-320.

Brandao, J. M. D. O. B., Almeida, N. S. M., Dixini, P. V. M., Baier, C. H. A., Dias, H. P., Bassane, J. F. P., Franca, H. S., Silva, S. R. C, Aquije, G. M. F. V., and Romao, W. (2016). Documentoscopy by atomic force microscopy (AFM) coupled with Raman microspectroscopy: Applications in banknote and driver license analyses. *Analytical Methods, 8(4),* 771-784. https://doi.org/10.1039/c5ay03128a

Cheng, D., Shi, Z., Tan, X., Zhu, Z., Jiang, Z., and Nmf, A. (2010). A Method of Automatically Estimating the Regularization Parameter for Non -negative Matrix Factorization. *Icnc,* 22-26.

Daniel.D, L., and Seung, S. (1999). Learning the parts of objects by non -negative matrix factorization. *Nature, 401(6155),* 788-791.

de Almeida, M. R., Correa, D. N., Rocha, W. F. C, Scafi, F. J. O., and Poppi, R. J. (2013). Discrimination between authentic and counterfeit banknotes using raman spectroscopy and PLS -DA with uncertainty estimation. *Microchemical Journal, 109,* 170 -177. https://doi.Org/10.1016/j.microc.2012.03.006

Dikbas, F. (2017). A novel two - dimensional correlation coefficient for assessing associations in time series data. *International Journal of Climatology ,* 37(11), 4065 -4076. https://doi.org/10.1002/joc.4998

Downes, A. (2019). Wide area Raman spectroscopy. *Applied Spectroscopy Reviews, 54(5),* 445-456. https://doi.org/10.1080/05704928.2019.1576190

Eleje P.E., CO. Buari, B. I. C. Maduagwu. and Abdulmalik, A. (2018). *COD 2018* Annual

Report. *Central Bank of Nigeria, pp 12*

Gierlinger, N., Luss, S., Konig, C, Konnerth, J., Eder, M., and Fratzl, P. (2010). Cellulose microfibril orientation of Picea abies and its variability at the micron -level determined by Raman imaging. *Journal of Experimental Botany , 61(2),* 587 -595. https.V/doi.org/l 0.1093/jxb/erp325

Gordon, K. C, and McGoverin, C. M. (2011). Raman mapping of pharmaceuticals. *International Journal of Pharmaceutics , 417*(1-2), 151 -162. https.V/doi.org/l 0.1016/j.ijpharm.2010.12.030

Guedes, A., Algarra, M., Prieto, A. C, Valentim,

B., Hortelano, V., Neto, S., Algarra, R., and Noronha, F. (2013). Raman microspectroscopy of genuine and fake euro banknotes. *Spectroscopy Letters , 46(S),* 569 -576. https://doi.org/10.1080/00387010.2013.769007

Guo, H., Yin, B., Zhang, J., Quan, Y., and Shi, G. (2016). Forensic classification of counterfeit banknote paper by X-ray fluorescence and multivariate statistical methods. *Forensic Science International , 266,* e43 -e47. https://d0i.0rg/l 0.1016/j.forsciint.2016.06.008

Hana V, P avel. T. and M ilan. S. (2019). *Application of Raman Spectroscopic Measurement for Banknote Security Purposes* (P. B. and A. C. Klimis Ntalianis, George Vachtsevanos (ed.); pp. 42 - 47). **https://doi.org/https://doi.org/10.1007/978-3-**030-21507-17

He, C, Girolami, M., and Ross, G. (2004). Employing optimized combinations of one -class classifiers for automated currency validation. *Pattern Recognition, 37(6),* 1085-1096. https.V/doi.org/l 0.1016/j.patcog.2004.02.002

Jaukovic, G. (2019). *Advantages and Disadvantages of Raman Spectroscopyiln Testing Paper. 6168,* 226-229.

Jones, K., Benson, S., and Roux, C. (2013). The forensic analysis of office paper using carbon isotope ratio mass spectrometry. Part 3: Characterizing the source materials and the effect of production and usage on the 513C values of paper. *Forensic Science International,* 255(1-3), 355-364. https://doi.Org/10.1016/j.forsciint.2013.10.011

Katarina, I., Marina, V., and Dubravco, B. (2018). FT-1R Spectroscopy as a discrimination Method for Establishing Authenticity of Euro Banknotes. *Acta Graphic, 29(2),* 27-30.

Lawandy, N. M., & Smuk, A. Y. (2014). Supercritical fluid cleaning of banknotes. *Industrial and Engineering Chemistry Research ,* 55(2), 530 -540. https://doorg/10.1021/ie403307y

Marabello, D., Benzi, P., Lombardozzi, A., and Strano, M. (2017). X -ray Powder Diffraction for Characterization of Raw Materials in Banknotes. *Journal of Forensic Sciences, 62(4).* https://doi.org/10.llll/1556-4029.13392

Miron, S., Dossot, M., Carteret, C, Margueron, S., and Brie, D. (2011). Joint processing of the parallel and crossed polarized Raman spectra and uniqueness in blind nonnegative source separation. *Chemometrics and Intelligent Laboratory Systems ,* 705(1), 7-18. https://doi.Org/10.1016/j.chemolab.2010.10.005

Muhammad, A. A. and Abba. B. (2017). Image -Base processing of Naira Currency Recognition. *Anale. Seria Informatica,* 75(1), 169-173.

Novais, A. R., Luiz, R, Roberto, C, and Neris, E. (2019). Characterization of Brazilian banknotes using portable X -ray fl uorescence and Raman spectroscopy. *Forensic Science International 302,*

109872. https://doi.Org/10.1016/j.forsciint.2019.06.030

Richard-Lacroix, M., and Pellerin, C. (2013). Accurate new method for molecular orientation quantification using polarized raman spectroscopy. *Macromolecules,* 4(5(14), 5561-5569. https://doi.org/10.1021/ma400955u

Shahdan, P. (1961). Permutation Ordering and Identification. *Mathematics Magazine , 34(6),* 353-358. https://doi.org/10.1080/0025570X.1961.11975264

Shin, K., and Chung, H. (2013). Wide area coverage Raman spectroscopy for reliable quantitative analysis and its app lications. In *Analyst* (Vol. 138, Issue 12, pp. 3335 -3346). Royal Society of Chemistry, https://doi.org/10.1039/c3an36843b

Sonnex, E., Almond, M. J., Baum, J. V., and Bond, J. W. (2014). Identification of forged Bank of England £20 banknotes using IR spectroscopy. *Spectrochimica Acta - Part A: Molecular and Biomolecular Spectroscopy* ,775,1158 -1163. https://doi.Org/10.1016/j.saa.2013.09.115

Svenningsson, L., Lin, Y. C, Karlsson, M., Martinelli, A., & Nordstierna, L. (2019).
Molecular Orientation Distribution of Regenerated Cellulose Fibers Investigated with Polarized Raman
Spectroscopy [Research -article]. *Macromolecules,* 52(10), 3918-3924. https://doi.org/10.1021/acs.macromol.9b00520

Takalo, J., Timonen, J., Sampo, J., Rantala, M., Siltanen, S., and Lassas, M. (2014). Using the fibre structure of paper to determine authenticity of the documents: Analysis of transmitted light images of stamps and banknotes. *Forensic Science International* , *244,* 252-258. https://doi.Org/10.1016/j.forsciint.2014.09.002

Tian, Y., and Zhang, Y. (2022). A comprehensive survey on regularization strategies in machine learning. *Information Fusion* , #0(October 2021), 146 -166. https://doi.Org/10.1016/j.inffus.2021.ll.005

Wang, J., Tian, F., Wang, X., Yu, H., Liu, C. H., and Yang, L. (2012). *Multi-Component Nonnegative Matrix Factorization.* 2922-2928.

Workman, J. (2001). Infrared and Raman spectroscopy in paper and pulp analysis. *Applied Spectroscopy Reviews, 36(2-3),* 139-168. https://doi.org/10.1081/ASR-100106154

Zhang, P., Wang, G., Zhang, X., and Li, Y Q. (2020). Single -Acquisition 2-D Multifocal Raman Spectroscopy Using Compressive Sensing. *Analytical Chemistry, 92(\),* 1326-1332. https://doi.org/10.1021/acs.analchem.9b04495

Zimmerley, M., Younger, R., Valenton, T., Oertel, D. C, Ward, J . L., and Potma, E. 0. (2010). Molecular orientation in dry and hydrated cellulose fibers: A coherent anti stokes Raman scattering microscopy study. *Journal of Physical Chemistiy B,* 774(31), 10200-10208. https://doi.org/10.1021/jpl03216j